



University of HUDDERSFIELD

University of Huddersfield Repository

Tesfa, Belachew, Mishra, Rakesh, Zhang, Cuiping, Gu, Fengshou and Ball, Andrew

NOx Prediction Based on Cylinder Pressure Measurement for Engine Emission Monitoring

Original Citation

Tesfa, Belachew, Mishra, Rakesh, Zhang, Cuiping, Gu, Fengshou and Ball, Andrew (2011) NOx Prediction Based on Cylinder Pressure Measurement for Engine Emission Monitoring. In: Proceedings of the 24th International Congress on Condition Monitoring and Diagnostics Engineering Management. COMADEM, Norway, p. 212. ISBN 0954130723

This version is available at <http://eprints.hud.ac.uk/9675/>

The University Repository is a digital collection of the research output of the University, available on Open Access. Copyright and Moral Rights for the items on this site are retained by the individual author and/or other copyright owners. Users may access full items free of charge; copies of full text items generally can be reproduced, displayed or performed and given to third parties in any format or medium for personal research or study, educational or not-for-profit purposes without prior permission or charge, provided:

- The authors, title and full bibliographic details is credited in any copy;
- A hyperlink and/or URL is included for the original metadata page; and
- The content is not changed in any way.

For more information, including our policy and submission procedure, please contact the Repository Team at: E.mailbox@hud.ac.uk.

<http://eprints.hud.ac.uk/>

NO_x Prediction Based on Cylinder Pressure Measurement for Engine Emission Monitoring

Belachew TESFA¹, Rakesh MISHRA¹, Cuiping ZHANG² Fengshou GU¹, Andrew BALL¹,

¹School of Computing and Engineering, University of Huddersfield, Huddersfield, HD1 3DH, UK

² Department of Vehicle Engineering Taiyuan University of Technology, Taiyuan, 030024, China

b.c.tesfa@hud.ac.uk, r.mishra@hud.ac.uk, f.gu@hud.ac.uk andrew.ball@hud.ac.uk,

ABSTRACT

Meeting European NO_x emission standards is one of the biggest challenges facing automotive industries. The available technologies to measure NO_x emission are dependent on measurement of different NO_x species. In addition, in most cases it requires conversion of other NO_x species to NO for measurement purposes. The ability to measure NO_x emission on-line during the transient engine operation may be very difficult due to the delay in reaction time in the NO_x measuring apparatus. NO_x emissions in compression ignition (CI) engines are largely a thermal phenomena thus cylinder pressure is key to making accurate predictions of NO_x. If cylinder pressure data is available the heat release during combustion can be modeled and thus NO_x emission can be more accurately simulated. Therefore, the main objective of this study is to investigate the performance of the cylinder pressure in predicting the NO_x emission from a CI engine running with biodiesel during both steady and transient operations. To address the problem experimental work has been conducted on a four-cylinder, four-stroke, direct injection (DI) and turbocharged diesel engine. In this investigation, biodiesel (produced from the rapeseed oil by transesterification process) has been used. During the experiment the in-cylinder pressure, TDC mark, fuel flow rate, air flow rate and the NO_x emission were measured. The temperature within the cylinder was predicted using the cylinder pressure. Using the temperature values the NO_x emission was simulated in Zeldovich extended mechanism. The measured and simulation results of NO_x emission were compared during steady state conditions and shows maximum error of 4.5%.

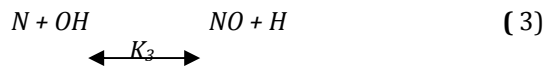
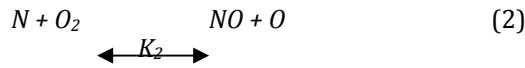
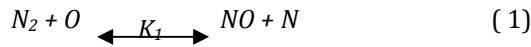
Keywords : NO_x emission, In-Cylinder Pressure, In-Cylinder Temperature, Biodiesel

1. INTRODUCTION

Oxides of Nitrogen are one of the most undesirable pollutant constituents of automotive transport because of its connection with the formation of photochemical smog in the atmosphere. It is also the major toxic emission that are being regulated with both in EU and USA emission regulations becoming more and more stringent (Aithal 2010); Dieselnets 2010; (C. Lin & H. Lin 2006).

NO_x formation pathway includes three methods, i.e., thermal NO_x, fuel NO_x, and prompt NO_x. Even though the degree of the emission release amount varies, each of the three pathways of NO_x formation contributes to the overall NO_x emission to the environment (Fuent, Inc 2003; Fernando et al. 2006). The thermal NO_x, is the main contributor to NO_x emissions from a diesel engine. It is formed during fuel combustion in the combustion cylinders when the atmospheric oxygen and nitrogen combine at a high temperature (Kornbluth et al. 2009; Troglor et al. 1997; K & M 2009). The general equation for the formation of NO_x can be described by equations (1-3) as described as the Zeldovich extended mechanism (Newhall 1969). To analysis the phenomena of NO_x generation in diesel engine, detailed knowledge of

the temperature and reaction mechanisms for fuel pyrolysis, NO_x, and unburnt carbon –hydrogen formation in the engine cylinder during the compression and power strokes (Mellor et al. 1998; Aithal 2010) are required.



The currently available methods of measuring/predicting NO_x emissions include analyzer (direct measuring), engine map method, and artificial neural network. Measurement of Oxides of nitrogen on a dry basis, by means of a heated chemiluminescent detector (HCLD) with a NO₂/NO analyzer is widely used. However, the analyzer has disadvantages of higher associated costs, requiring large space, demanding frequent calibration and possible effects of soot. In addition, its responses are very slow, which affect the transient NO_x emission measurement (Krijnsen et al. 1999). However, the formation of NO is the most significant phenomena under transient engine operations. This effects are mainly seen during engine acceleration or load acceptance, owing to the momentary increase in fuel injection which contributes to higher cycle temperatures and, hence NO production (Armas et al. 2006; Samuel et al. 2007). An engine map is a NO_x database generally based on measurements of a series of settings of engine speed and torque or power of the engine under stationery conditions. Most of the maps have the disadvantages that the map does not consider all the significant variables on the NO_x emission levels. This may cause deviations between the real NO_x emissions estimated from the engine map. In addition, it will estimate the transient conditions from the discrete steady state values (Krijnsen et al. 1999). The third method which needs the artificial neural network (ANN) system has advantage of avoiding in using the NO_x emission models, and work with transient conditions. However, in the neural network there is no explicit mathematical representation of the physical process and the predicting capability is limited only to specific engine type for which the neural network trained (S H Chan 1999).

The in-cylinder pressure measurement is considered a very valuable source of information during the development, testing and condition monitoring stages of engine development (Payri et al. 2010). NO_x emission in CI engines is largely a thermal phenomenon and thus cylinder pressure can be used to make an accurate prediction of NO_x quantity in real time, which will utilize of in-cylinder measurement. Therefore the main objective of this study is to investigate a novel approach to using the cylinder pressure for predicting the NO_x emission of a CI engine running with biodiesel during both steady and transient operations.

2. MODEL FORMULATION

The main task of this study is to use the in-cylinder pressure measurement to predict the NO_x emission from the CI engine. Generally, it has been well established the dominate process that produces NO in CI engine combustion. It is the thermal mechanism, which occurs in the post-flame burned gases, and described by the extended Zeldovich mechanism which described by equations (1-3) including the reactants, products and rate constants. In order to drive the rate of change of NO concentration, it was assumed that the concentration of the N is minor in comparison with the concentrations of the other species, so that the rate of change in N can be set equal to zero. Using this assumption and after some mathematical rearranging the rate of NO concentration, denoted as [NO], is given by equation (4).

$$\frac{dNO}{dt} = 2k_1[O][N_2] \frac{\left(1 - \frac{k_{-1}k_{-2}[NO]^2}{k_1[N_2]k_2O_2}\right)}{\left(1 + \frac{k_{-1}[NO]}{k_2[O_2] + k_3[OH]}\right)} \quad \text{g mol}/(\text{m}^3 \text{ s}) \quad (4)$$

The rate constants for these reactions have been measured in numerous studies and critically evaluated (Mellor et al. 1998; Aithal 2010; Fuent, Inc 2003), and the reaction rates used in this NO_x model

are given in Table (1). In Table 1 the (-) sign indicate the backward reaction. The $[N_2]$ and $[O_2]$ concentrations were determined at ambient condition of the atmospheric air.

Table 1 Rate constants for thermal NOx formation (Fuent, Inc 2003)

Rate constants	Values $[(m^3/(gmol. s))]$
k_1	$1.8 \times 10^8 e^{-\frac{38370}{T}}$
k_{-1}	$3.8 \times 10^7 e^{-\frac{425}{T}}$
k_2	$1.8 \times 10^4 T e^{-\frac{4680}{T}}$
k_{-2}	$3.8 \times 10^3 T e^{-\frac{20820}{T}}$
k_3	$7.1 \times 10^8 e^{-\frac{450}{T}}$
k_{-3}	$1.7 \times 10^8 e^{-\frac{24560}{T}}$

The concentration of oxygen $[O]$ by equation (5) and (6) and the maximum value was taken. Similarly, the $[OH]$ was estimated by equation (7).

$$[O] = 3.97 \times 10^5 T^{-1/2} [O_2]^{1/2} e^{-31090/T} \quad \text{g mol/m}^3 \quad (5)$$

$$[O] = 36.64 T^{1/2} [O_2]^{1/2} e^{-27123/T} \quad \text{g mol/m}^3 \quad (6)$$

$$[OH] = 2.129 \times 10^2 T^{-0.57} [O_2]^{1/2} [H_2O]^{1/2} e^{-4595T} \quad \text{g mol/m}^3 \quad (7)$$

To predict the thermal NOx emission from the in-cylinder temperature the ideal-gas equation of state which described in equation (8) was used.

$$T(\theta) = \frac{P(\theta)V(\theta)}{Ma(\theta)R_g} \quad (8)$$

Where, $T(\theta)$ is the instantaneous in-cylinder temperature(K), $P(\theta)$ is the instantaneous in-cylinder pressure(Pa), $M(\theta)$ is the instantaneous mass in cylinder (kg), R_g is gas constant (J/kg-K) and $V(\theta)$ is the instantaneous cylinder volume (M^3) calculated by equation (9).

$$V(\theta) = \frac{V_d}{\gamma_c - 1} + \frac{V_d}{2} [R + 1 - \cos\theta - (R^2 - \sin^2\theta)^{1/2}] \quad (9)$$

Where V_d is displacement volume given R is the ratio of connecting rod length to crank radius and r_c is compression ratio.

The model was simulated numerically using a Matlab program under different engine operation conditions explained in section 3.

3. EXPERIMENTAL FACILITIES AND TEST PROCEDURE

In this study the in-cylinder pressure, fuel mass flow rate, air flow rate and NO_x emission were measured and used in the NO_x prediction model and for validation purposes. The engine used in the present investigation is a four-cylinder, four-stroke, turbo-charged, water-cooled and direct-injection CI engine. Full details of parameters of the engine are included in table 2. The load to the engine was provided by a 200kW AC Dynamometer with 4-Quadrant regenerative drive with motoring and absorbing capability for both steady and transient conditions. It is integrated with speed sensors, pressure transducers, thermocouples, air flow meters, fuel flow meters and in-line torque meter. A Hengler RS58 speed sensor was used to measure the speed of the engine. The air-consumption was measured using hot-film air-mass meter HFM5 and the fuel consumption was measured by FMS-1000 gravimetric fuel measuring which was controlled and monitored by CADETV12 software. The cylinder pressure was measured using Kistler 6125A11 model air-cooled piezo-quartz pressure sensor which was mounted on the cylinder head. The cylinder pressure signal was passed through Bruel & Kjaer 2635 charge amplifier. The crankshaft position was obtained using a crank angle sensor to determine the cylinder pressure as a function of the crank angle.

All the signals collected from the test rig needed to be converted from an original analogue form to a digital form. This was achieved by using a Cambridge Electric Design (CED) Power 1401 Analogue to Digital Converter (ADC) interface between the transducers and the computer. The Analogue to Digital Converter (ADC) has 16 channels and 500 MHz bandwidth. The fuel from biodiesel tank was pumped to a fuel meter and, then it was passed through a fuel pump to the fuel injectors. The scheme of the test rig layout with the basic instrumentations is shown in figure 1.

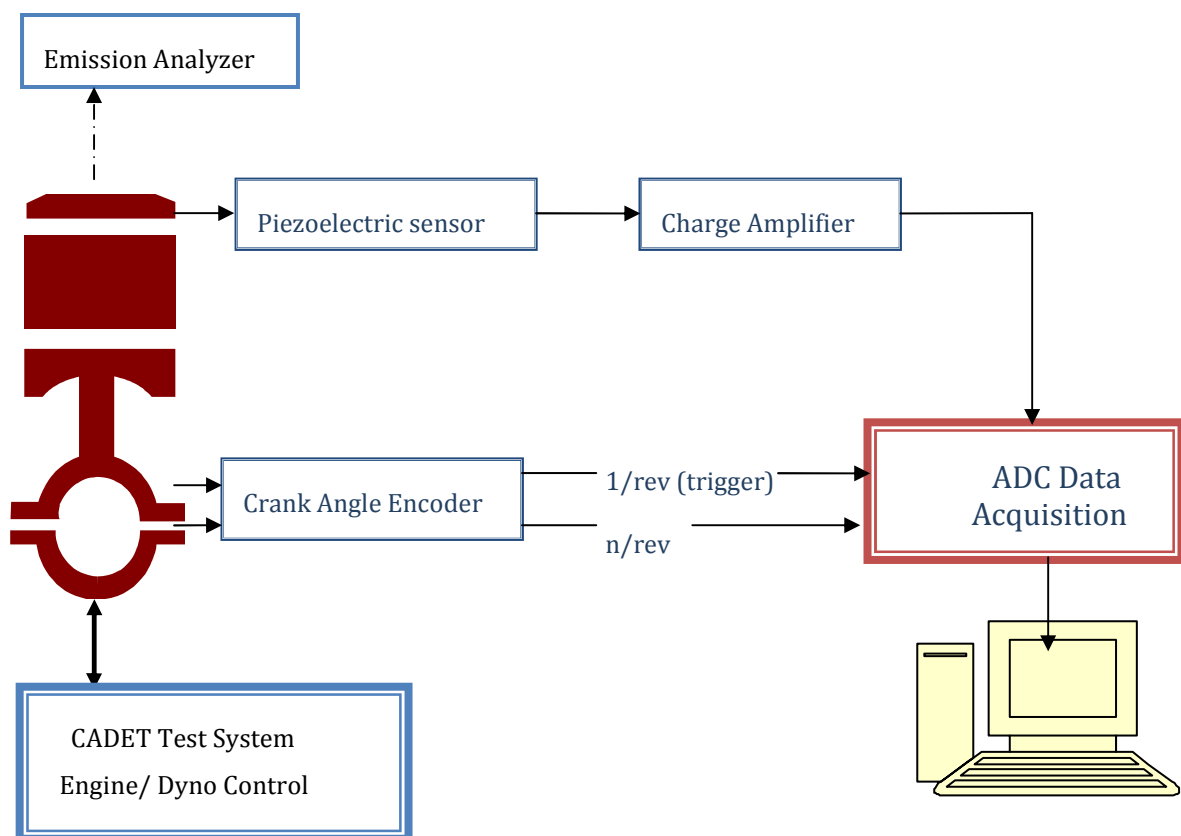


Figure 1 Experimental setup

The measurement of the gaseous emissions was carried out using a gas test bench HORIBA, Horriba EXSA - 1500. It has measuring range of 0 - 5000ppm and an error of 1%. The sample line of the equipment is connected directly to the exhaust pipe and it is heated to maintain a wall temperature of around 191°C and avoid condensation of hydrocarbons. The insulated line is extended from the exhaust pipe to the

equipment unit where the analyzers are located. Oxides of nitrogen are measured on a dry basis, by means of a heated chemiluminescent detector (HCLD) with a NO₂/NO converter.

During the testing process the engine was initially run for 10 minutes to bring it to a steady state before any measurements were carried out. On the day prior to the actual test day and also in between test regimes with different fuel type, a preconditioning procedure was implemented that included running the engine at a high load and then at a low load to purge out any of the remaining effects from previous tests in the engine fuel system and also to remove the deposited hydrocarbon from the sample line. The frequency of the data acquisition system was 37kHz. The sampling time used was 40 seconds. The operating conditions used in the tests are listed on Table 3. The operating conditions were selected with an aim to cover main engine operating speeds and loads as per the New European Driving Cycle (NEDC).

Table 2 Characteristics of engine

Parameters	Specification
Engine type	Turbo charged diesel engine
Number of cylinders	4
Bore	103mm
Stroke	132mm
Compression ratio	18.3
Number of valves	16
Injection system	Direct injection
Displacement	4.399 liter
Cooling system	Water

Table 3 Operating conditions

Condition	Speed(rpm)	Load(Nm)	Fuel
A	900	105, 210, 315, 420	Diesel, Biodiesel
B	1100	105, 210, 315, 420	Diesel, Biodiesel
C	1300	105, 210, 315, 420	Diesel, Biodiesel
D	1500	105, 210, 315, 420	Diesel, Biodiesel

The biodiesel used in this study was rapeseed oil biodiesel purchased from a local biodiesel producer. The biodiesel was produced by transesterification process from 'virgin' oil using methanol. The main physical properties such as composition, density, lower heating value and viscosity of the biodiesel were measured in the applied science laboratory according to the official test standards and are shown in Table 4.

Table 4 Physical and Chemical properties of fuel

Property	Units	Diesel	Biodiesel
Composition	% C	87	77
	% H	13	12
	% O	0	11
Density	Kg m ⁻³	853	879
Lower heating value(LHV)	MJ Kg ⁻¹	42679	38500
Viscosity , mm ² /s	mm ² s ⁻¹	3.55	5.13

4. RESULT AND DISCUSSION

To predict the NO_x emission from the measured in-cylinder pressure using ideal-gas state equation, the in-cylinder pressure and the in-cylinder temperature characteristics of the combustion are described. The comparison of the in-cylinder pressure and in-cylinder temperature of diesel and biodiesel fuel are also discussed in detail. Finally the predicted NO_x emissions values from in-cylinder pressure measurement were compared with measured NO_x emission for both diesel and biodiesel fuel.

Figure 2(a) shows that the in-cylinder pressure within the combustion chamber of the CI engine running with 100B (100% Bio-diesel) at a speed of 1300 rpm and engine loads of 105Nm, 210Nm, 315Nm and 420Nm. The results show that the peak cylinder pressure of the engine increases with increasing the load from 105Nm to 420Nm.

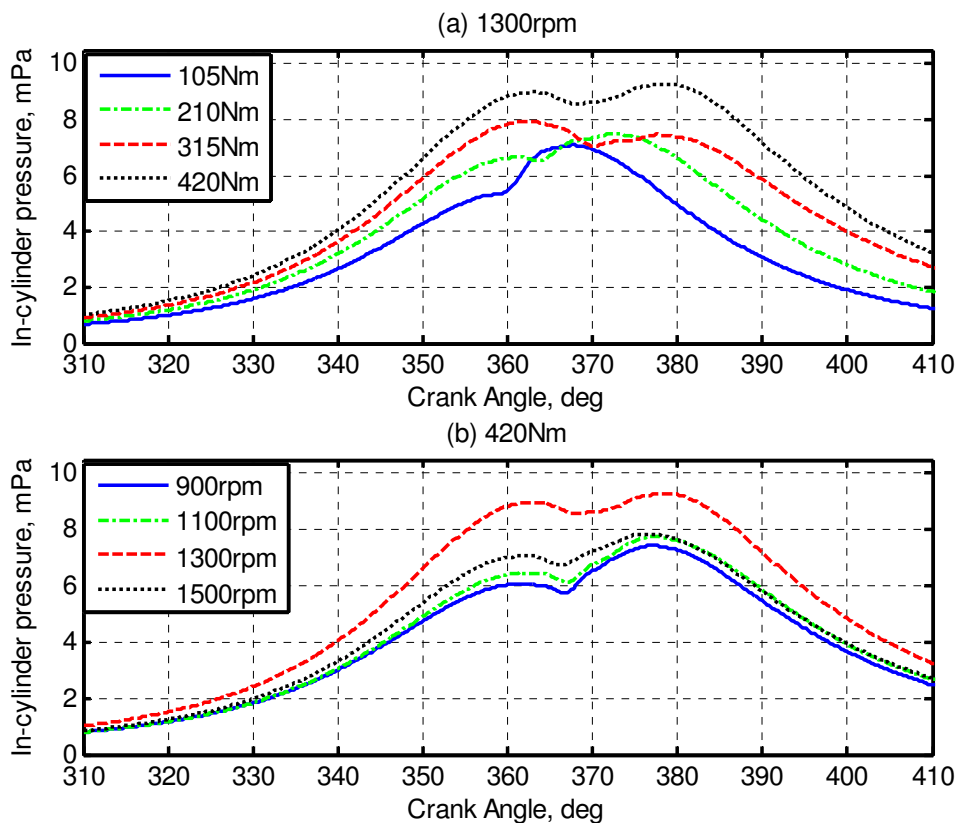


Figure 2 In-cylinder pressure at different crank angle (a) at 1300 rpm and various load (b) at 420Nm and various engine speed.

The cylinder produces the minimum peak in-cylinder pressure of 6.5MPa at 105Nm and the maximum in-cylinder pressure of 8.8 MPa at 420Nm. The effects of the engine speed on the in cylinder pressure within the combustion chamber of the CI engine running with 100B at a load of 420Nm and various engine speeds are depicted in figure 2(b). The results show that the peak of cylinder pressure of the engine increases with increasing the engine speed.

The biodiesel combustion flame temperature values, which have been calculated from the instantaneous in-cylinder pressure, cylinder volume and air flow rate, are depicted in figure 3(a) and figure 3(b) for different engine speeds and loads ranges respectively. It can be seen, in figure 3(a), that when the load increases the in-cylinder temperature also increases. Similarly, when the engine speed increases the in-cylinder pressure also increases. It can be concluded from the above that when the engine speed and load increase the in-cylinder pressure increases. Even though, the cylinder volume and cylinder pressure are inversely proportionally, since the change magnitude of the in-cylinder pressure is higher, its effect dominate the in-cylinder temperature values. In Figure 3(b) it can be seen that generally the in-cylinder temperature increases with increasing the speed up to engine speed of 1300rpm.

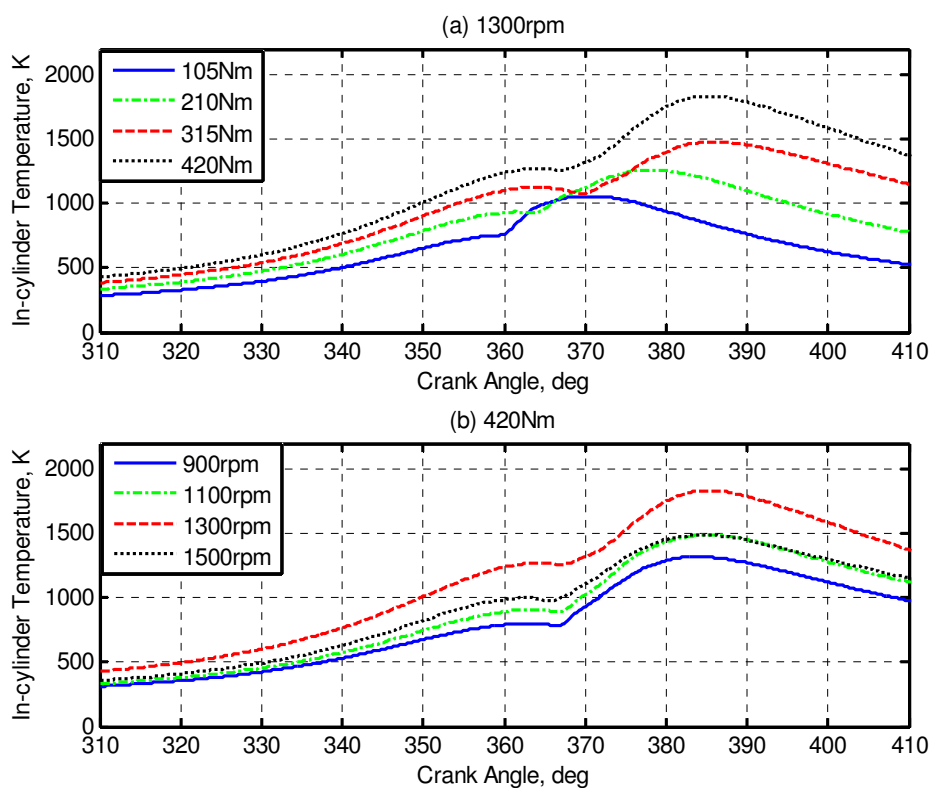


Figure 3 In-cylinder temperature at different crank angle (a) at 1300 rpm and various load (b) at 420Nm and various engine speed.

Figure 4 shows that the in-cylinder pressure within the combustion chamber of the CI engine running with diesel and 100B at different engine speeds and engine load of 420Nm. The results show that the peak cylinder pressure of the engine running with biodiesel is slightly higher than the engine running with diesel. The main cause for higher peak in-cylinder pressure in the CI engine running with biodiesel is because of the advanced combustion process initiated by easy flow-ability of bio-diesel due to the physical properties of the biodiesel. In addition, due to the presence of oxygen molecule in the biodiesel, the hydrocarbons achieve complete combustion (Canakci 2007; Gumus 2010) resulting in higher in-cylinder pressure.

Figure 5 shows the in-cylinder temperature for biodiesel and diesel operating conditions. The result shows that the flame temperature corresponding to biodiesel operation is higher than the diesel operation. The higher temperature of the biodiesel is caused due to the availability of additional oxygen molecule as mentioned earlier. As it will be discussed later this is the main cause for the higher emission

of NOx. On the contrary Monyem et al (Monyem et al. 2001) reported that for both constant-volume combustion and constant-pressure combustion, the flame temperature for biodiesel is slightly below that for diesel fuel.

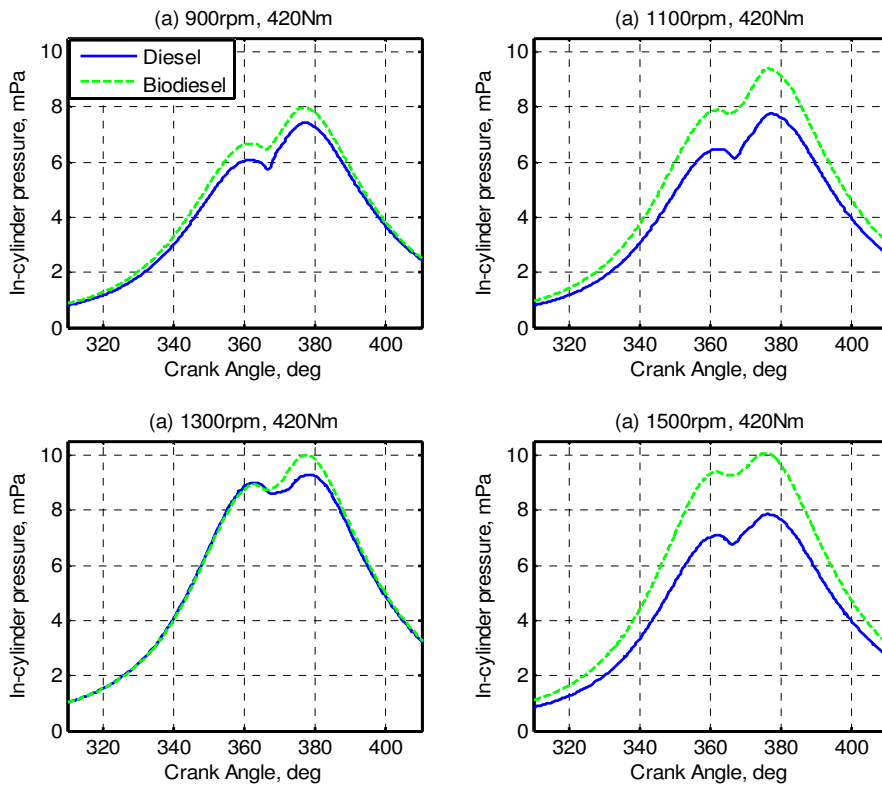


Figure 4 In-cylinder pressure of the CI engine running by biodiesel and diesel at 420Nm and different engine speed

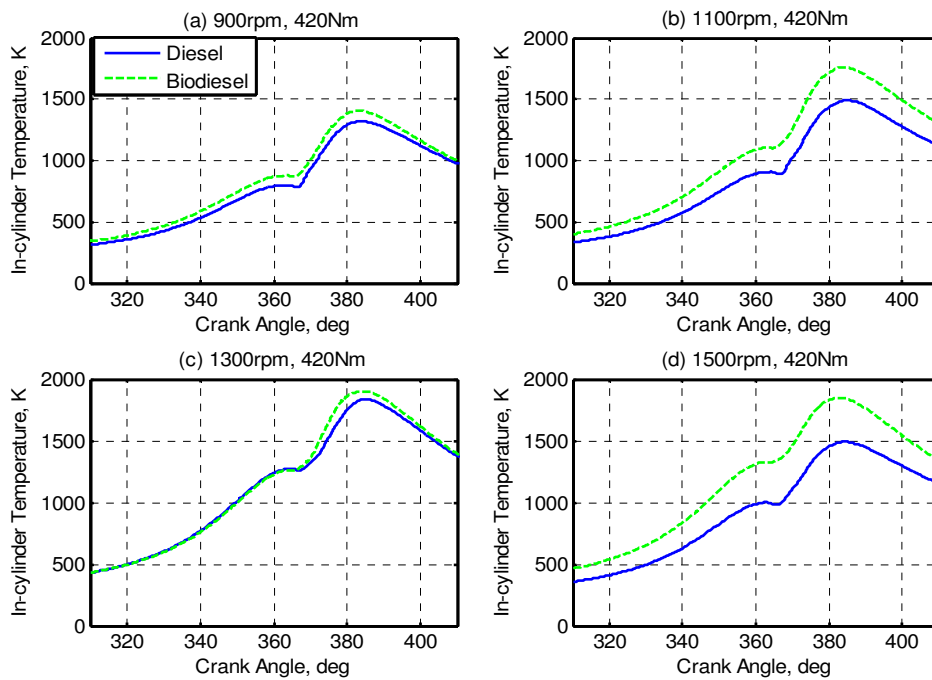


Figure 5 In-cylinder temperature of the CI engine running by biodiesel and diesel at 420Nm and different engine speed

The predicated NOx emission corresponding to the biodiesel operation at a load of 315Nm and various engine speeds are shown in figure 6. The NOx emissions were found to decrease with the increase in the

engine speed. This can be explained as at higher engine speed, the volumetric efficiency and gas flow motion within the engine cylinder are increased. These lead to faster mixing between air and fuel and minimize the ignition delay (C. Lin & Chen). As a result the nitrogen and oxygen molecule resident time is reduced.

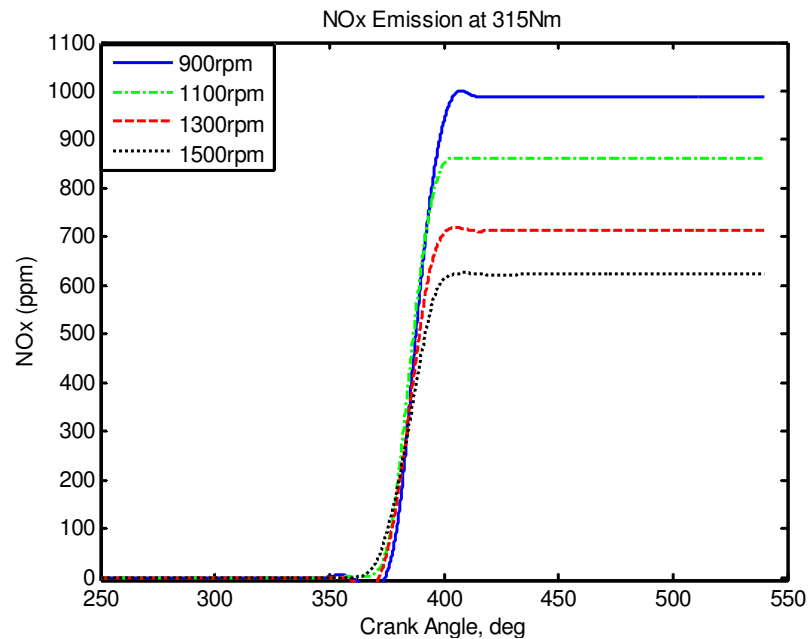


Figure 6 Predicted NOx emission at 315Nm and various engine speeds

Figure 7 shows the predicted value of nitrogen oxides (NOx) emission for engine running with biodiesel and diesel at 315Nm load for speed of 900rpm, 1100rpm, 1300rpm and 1500rpm. It can be seen that the NOx emission when running with biodiesel is higher than that of the diesel by 5, 10, 17 and 7 % respectively. The main reason for higher emission of biodiesel is the advanced combustion process initiated because of the physical properties of biodiesel (viscosity, density, compressibility, sound velocity) (Lapuerta et al. 2008; Wang et al. 2000). When biodiesel is injected, the pressure rise produced by the pump is quicker as a consequence of its lower compressibility (higher bulk modulus) and propagate more quickly towards the injectors. As a result, the cylinder gas becomes rich fairly quickly by fuel and reaches its peak temperature which speeds up the formation NOx.

To investigate the accuracy of the NOx prediction model from the cylinder pressure, the measured and the predicted value of NOx are presented in table 1. It can be seen from the table that maximum deviation of the model from the measured one is 4.06% for diesel and 4.39% for biodiesel.

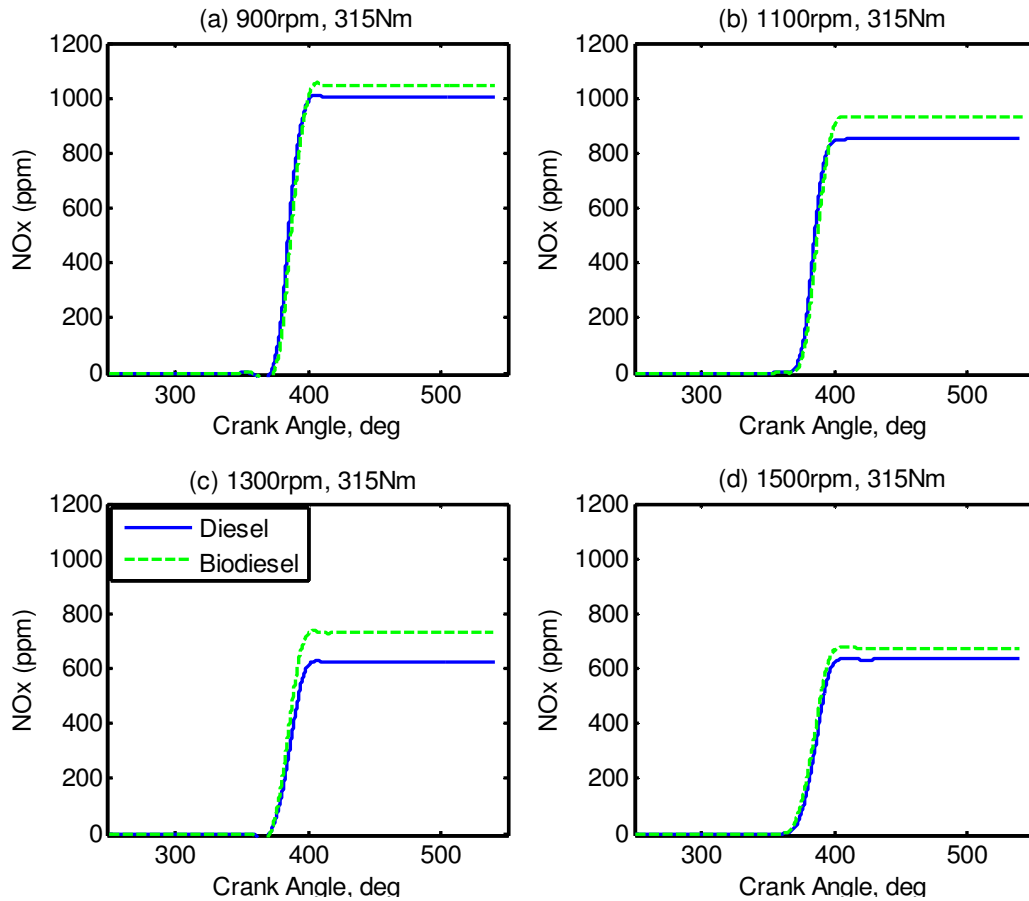


Figure 7 Predicted NOx emission of biodiesel and diesel at 315Nm and various engine speeds

Table 5 Measured and Predicted NOx emission values at 315Nm

Speed(rpm)	Diesel(ppm)		Biodiesel(ppm)		Diesel Deviation	Biodiesel Deviation
	Measured	Predicted	Measured	Predicted		
900	1020	1002	1050	1094	1.76	-4.39
1100	850	850	910	896	0.00	1.65
1300	715	686	730	719	4.06	1.60
1500	615	637	670	660	-3.58	1.57

CONCLUSION

In this study, the performance of using the cylinder pressure to predict the NOx emission has been investigated based on a compression ignition (CI) engine running with different fuels including biodiesel. The temperature of the cylinder is predicted firstly using the cylinder pressure by ideal-gas state equation. Using the predicted temperature the NOx emission is then calculated based the Zeldovich extended mechanism. The measured and prediction results of NOx emission are compared and it has been shown that the deviation of the values obtained from the model from the measured values is less than to 4.06% for diesel and 4.39% for biodiesel respectively. Moreover, the reasons for higher NOx emission

from biodiesel have been explored based on the predication. The prediction paves the way of real-time NOx emission estimation for engine transient study and on-line diagnosis.

Reference

- Aithal, S., 2010. Modeling of NOx formation in diesel engines using finite-rate chemical kinetics. *Applied Energy*, 87(7), 2256-2265.
- Armas, O., Hernández, J.J. & Cárdenas, M.D., 2006. Reduction of diesel smoke opacity from vegetable oil methyl esters during transient operation. *Fuel*, 85(17-18), 2427-2438.
- Canakci, M., 2007. Combustion characteristics of a turbocharged DI compression ignition engine fueled with petroleum diesel fuels and biodiesel. *Bioresource Technology*, 98(6), 1167-1175.
- Fernando, S., Hall, C. & Jha, S., 2006. NOx Reduction from Biodiesel Fuels. *Energy & Fuels*, 20(1), 376-382.
- Fuent, Inc, 2003. Thermal NOx Formation. Available at: <http://jullio.pe.kr/fluent6.1/help/html/ug/node624.htm> [Accessed August 19, 2010].
- Gumus, M., 2010. A comprehensive experimental investigation of combustion and heat release characteristics of a biodiesel (hazelnut kernel oil methyl ester) fueled direct injection compression ignition engine. *Fuel*, 89(10), 2802-2814.
- K, K. & M, U., 2009. Modeling of Nitric Oxide Formation in Single Cylinder Direct Injection Diesel Engine Using Diesel-Water Emulsion. *American Journal of Applied Sciences*, 6(7), 1313-1320.
- Kornbluth, K., McCaffrey, Z. & Erickson, P.A., 2009. Incorporating in-cylinder pressure data to predict NOx emissions from spark-ignition engines fueled with landfill gas/hydrogen mixtures. *International Journal of Hydrogen Energy*, 34(22), 9248-9257.
- Krijnsen, H.C. et al., 1999. Prediction of NOx Emissions from a Transiently Operating Diesel Engine Using an Artificial Neural Network. *Chemical Engineering & Technology*, 22(7), 601-607.
- Lapuerta, M., Armas, O. & Rodríguez-Fernández, J., 2008. Effect of biodiesel fuels on diesel engine emissions. *Progress in Energy and Combustion Science*, 34(2), 198-223.
- Lin, C. & Chen, L., Engine performance and emission characteristics of three-phase diesel emulsions prepared by an ultrasonic emulsification method. *Fuel*, 85(5-6), 593-600.
- Lin, C. & Lin, H., 2006. Diesel engine performance and emission characteristics of biodiesel produced by the peroxidation process. *Fuel*, 85(3), 298-305.
- Mellor, A. et al., 1998. Skeletal Mechanism for NOx Chemistry in Diesel Engines. *SAE*, (981450). Available at: <http://papers.sae.org/981450/> [Accessed December 10, 2010].

- Monyem, A., Van Gerpen, J. & Cankci, M., 2001. The Effects of Timing and Oxidation on Emissions from biodiesel-Fueled Engines. *Transactions of the ASAE*, 44(1), 35-42.
- Newhall, H.K., 1969. Kinetics of engine-generated nitrogen oxides and carbon monoxide. *Symposium (International) on Combustion*, 12(1), 603-613.
- Payri, F. et al., 2010. Digital signal processing of in-cylinder pressure for combustion diagnosis of internal combustion engines. *Mechanical Systems and Signal Processing*, 24(6), 1767-1784.
- Samuel, S. et al., 2007. Parametric Study into the Effects of Factors Affecting Real-World Vehicle Exhaust Emission Levels. *SAE*, (2007-01-1084). Available at: <http://papers.sae.org/2007-01-1084/> [Accessed December 10, 2010].
- Trogler, W.C., Bruner, E. & Westwood, G., 1997. Kinetics of the Reaction Between Nitric Oxide and Oxygen. An Interactive Laboratory Experiment. Available at: <http://chem-faculty.ucsd.edu/trogler/CurrentNitroWeb/Section3/section4.html> [Accessed August 19, 2010].
- Wang, W. et al., 2000. Emissions from Nine Heavy Trucks Fueled by Diesel and Biodiesel Blend without Engine Modification. *Environmental Science & Technology*, 34(6), 933-939.